Microstructure and Isotopic Labeling Effects on the Miscibility of Polybutadiene Blends Studied by the Small-Angle Neutron Scattering Technique

Shinichi Sakurai,† Hirokazu Hasegawa, and Takeji Hashimoto

Department of Polymer Chemistry, Faculty of Engineering, Kyoto University, Kyoto 606, Japan

I. Glen Hargis and S. L. Aggarwal

Research Division, Gen Corp, Akron, Ohio 44305

Charles C. Han*

Polymers Division, National Institute of Standards and Technology, Gaithersburg, Maryland 20899. *Received March 30, 1989; Revised Manuscript Received June 15, 1989*

ABSTRACT: Deuterated polybutadiene and protonated polybutadiene (PBD/PBH) blends with various microstructures have been studied by the small-angle neutron scattering experiments. Correlation length, ξ, zero wavenumber structure factor, $S(q = 0)$, and interaction parameter, χ_{blend}, have been obtained. All PBD/PBH blends exhibit UCST behavior. With the use of random copolymer theory, the interaction parameter, χ_{blend}, has been successfully separated into χ_1, χ_2, and χ_3 which are interaction parameters between the same isotopically labeled 1,2-unit and 1,4-unit, the opposite isotopically labeled 1,2-unit and 1,4-unit, and the opposite isotopically labeled 1,2-unit and 1,2-unit or 1,4-unit and 1,4-unit, respectively.

I. Introduction

Polybutadiene blends of various microstructures are widely used in the rubber industry to tailor the properties to the applications.[1] Such blends offer an ideal system to study the fundamentals of binary interaction parameters of butadiene monomers with different microstructures.

Small-angle neutron scattering (SANS) should be the tool to use to study this microstructure effect.[2] Unfortunately, the deuterium labeling of one of the components that is needed for SANS introduces a repulsive interaction[3] between the two components. This has prevented a straightforward measurement of the binary interaction parameter, χ, between a 1,2-unit and a 1,4-unit.

In this paper, an attempt has been made to separate the isotope effect from the microstructure effect through a systematic SANS study of blends of deuterated polybutadiene (PBD) and protonated polybutadiene (PBH) with various vinyl content. Random copolymer theory[4-6] was used to carry out this separation. Although three versions of almost identical theories[4-6] on random copolymers have been published at about the same time, we have chosen to use the ten Brinke, Karasz, and MacKnight version for convenience in our application. Reasonable results have been obtained by using this analysis scheme indicating that the ten Brinke, Karasz, and MacKnight[4] calculation works well for the PBD/PBH blends.

We will present the sample characterization, specimen preparation, and SANS geometry in section II. Experimental results, data analysis procedures, spinodal temperatures, T_s, and interaction parameter, χ, will be presented together with phase diagram in section III. The procedure used to separate the microstructure contribution from isotope contribution to the total interaction parameter will be discussed in C and D of section III. Finally, we will give our conclusion in section IV.

II. Experimental Section

Two medium vinyl polybutadiene samples, VBRD6 and VBRH6, with about 65% 1,2-content, were synthesized by one of the authors (I.G. Hargis from Gen Corp) for this study. The VBRD6 is a perdeuterated polybutadiene that is similar to the normal protonated VBRH6 in characteristics. The detailed characterization is listed in Table I.

The other two PB samples, CisBR7k and CisBR150k, were also prepared by I. G. Hargis from Gen Corp by anionic polymerization. The detailed characterization is also listed in Table I.

Blends specimens were prepared by dissolving polymers in toluene and then cast (from approximately 5% concentration solution) into films. These polymer films were thoroughly dried under vacuum at room temperature for at least 1 day. Three pairs of polybutediene blends, VBRD6/VBRH6, VBRD6/CisBR7k, and VBRD6/CisBR150k, at various compositions were prepared. The compositions are listed in Table II. Miscibility of each specimen was checked by preliminary light scattering experiment. Specimens from the VBRD6/VBRH6 series and from the VBRD6/CisBR7k series were all miscible, but the specimens from the VBRD6/CisBR150k series were all phase separated with spinodal rings observed. Therefore, only VBRD6/VBRH6 and VBRD6/CisBR7k series were used for further SANS study. Light scattering results are also listed in Table II for each specimen.

Specimen disks of about 1 mm in thickness and about 13 mm in diameter were used for all SANS studies. The specimens were sandwiched between two oxygen free pure copper disk of about 0.22 mm in thickness and mounted in the heating block to ensure good temperature control. Small-angle neutron scattering experiments were carried out at the SANS facility of the NIST reactor. The instrument has been described elsewhere.[7] In this study, the focusing geometry with 6-Å neutron wavelength was used. Absolute scattering intensity for each specimen was obtained through use of a secondary standard of dry silica gel.[8] A copper heating block was used to control the specimen temperature to within 0.3 °C of desired temperature during measurement. Specimens were preheated at a given temperature for at least 30 min before the SANS measurements

† Present address: Department of Polymer Science and Engineering, Faculty of Textile Science, Kyoto Institute of Technology, Matsugasaki, Sakyo-ku, Kyoto 606, Japan.

0024-9297/90/2223-0451$02.50/0

Table I
Sample Characteristics

sample code	microstructure[a] 1,2	cis-1,4	trans-1,4	$10^{-3}M_n$	M_w/M_n[b] (GPC)	T_g, °C (DSC)
VBRD6	63	*	*	134[b]	2.0	-42 (PBD)
VBRH6	68	11	21	135[b]	1.8	-39 (PBH)
CisBR7k	7	40	53	6.9[c]	1.5	... (PBH)
CisBR150k	8	43	49	145[d]	1.8	... (PBH)

[a] Microstructure determined by ^{13}C NMR (%). The asterisk means cis and trans contents cannot be accurately determined owing to spectral broadening. [b] M_n and M_w/M_n determined by GPC (polystyrene equivalent). [c] Determined by vapor pressure osmometry. [d] Determined by osmometry.

Table II
Blends Preparation[a]

blend system	designatn	compn, ϕ[b]	turbidity	light scattering
VBRD6/VBRH6	30/70	0.278	clear	no scattering
	40/60	0.375	clear	no scattering
	50/50	0.474	clear	no scattering
	70/30	0.677	clear	no scattering
VBRD6/CisBR7k	10/90	0.092	clear	no scattering
	50/50	0.477	clear	no scattering
VBRD6/CisBR150k	50/50	0.477	turbid	spinodal ring observed

[a] All blend samples contain Irganox 565 as an antioxidant. [b] Volume fraction of VBRD6 in the blends.

were started. Most specimens were measured between room temperature and 180 °C at either 20 or 30 °C intervals. The detailed measurement temperatures will be given later together with experimental χ parameters.

III. Results and Discussion

A. Data Analysis. All SANS data are analyzed with nonlinear regression fitting routine[2] according to the random phase approximation calculation of deGennes[9] which can be written as follows (see Appendix A):

$$S(q) = k_N/\left[\frac{1}{\phi_A\langle Z_A\rangle_n v_A\langle g_D(q)_A\rangle_w} + \frac{1}{\phi_B\langle Z_B\rangle_n v_B\langle g_D(q)_B\rangle_w} - \frac{2\chi}{v_0}\right] \quad (1a)$$

with

$$S(q)_{exp} = S(q) + \text{base line} \quad (1b)$$

where $\langle Z_i\rangle_n$ is the number-averaged polymerization index for the ith component. $\langle g_D(q)_i\rangle_w$ is the weight-averaged Debye function for the ith component. Assuming a polydispersity with the Schultz–Zimm distribution,[10] then

$$\langle g_D(q)_i\rangle_w = \frac{2}{\langle x_i\rangle_n^2}\left[\langle x_i\rangle_n - 1 + \left(\frac{h_i}{h_i + \langle x_i\rangle_n}\right)^{h_i}\right]$$

with $\langle x_i\rangle_n \equiv q^2\langle Z_i\rangle_n b_i^2/6 = q^2\langle R_{gi}^2\rangle_n$ and $q \equiv 4\pi/\lambda \sin(\theta/2)$, where b_i is the statistical segment length of the ith component, θ is the scattering angle, λ is the wavelength of the neutron used, and $\langle R_{gi}\rangle_n$ is the number-averaged radius of gyration of the ith component. Also, $h_i \equiv (\langle Z_i\rangle_w/\langle Z_i\rangle_n - 1)^{-1}$, ϕ_i is the volume fraction of the ith component, and k_N is the contrast factor equal to $N_A(a_1/v_1 - a_2/v_2)^2$ with a_i as the scattering length of one monomer unit of the ith component, N_A as Avogadro's number, v_i is the molar volume of the ith component, and v_0 is the molar volume of a reference cell for the blend. If we assume the blends are incompressible, then $v_0 = (\phi_A/v_A + \phi_B/v_B)^{-1}$. With use of scattering lengths of -0.374×10^{-12}, 0.667×10^{-12}, and 0.665×10^{-12} cm/atom for H, D, and C, respectively,[11] the calculated scattering length per monomer for each polybutadiene sample used together with their molar volume and density are listed in Table III.

Table III
Scattering Length, Molar Volume, and Density

	$10^{12}a$, cm/monomer unit	v, cm^3/mol	ρ, g/cm^3
VBRD6	6.666	61.1	0.982[a]
VBRH6	0.4194	61.1	0.884[b]
CisBR7k	0.4194	60.4	0.895[b]

[a] This is estimated by assuming that the molar volume of the VBRD6 is the same as the VBRH6. [b] Fetters, L. J., private communication.

The above description of $S(q)$ is only an extension of the RPA calculation of deGennes[9] which can be obtained as shown in Appendix A by following Hong and Noolandi,[12] Rameau, Gallet, Marie, and Farnoux,[13] Ionescu, Picot, Duval, Duplessix, Benoit, and Cotton,[14] and Mori, Tanaka, Hasegawa, and Hashimoto.[15]

In all nonlinear regression fitting for SANS data to eq 1, three adjustable parameters, a single statistical segment length, b (setting the ratio $b_B/b_A = 1$ will be discussed later), interaction parameter, χ/v_0, and a baseline value, were used. The interaction parameter, χ/v_0, has thus been obtained for various compositions and temperatures for the series of specimens. It should be noted that the χ values which appear in the text and figures below were obtained as the products of χ/v_0 multiplied by v_0. The zero wavenumber scattering intensity, $S(q = 0)$, and the correlation length, ξ, have also been obtained for all corresponding conditions according to[2,9,16,17]

$$S(q=0) = k_N/\left[\frac{2}{v_0}(\chi_s - \chi)\right] \quad (2a)$$

with

$$\chi_s = \frac{v_0}{2}\left(\frac{1}{v_A\phi_A\langle Z_A\rangle_w} + \frac{1}{v_B\phi_B\langle Z_B\rangle_w}\right) \quad (2b)$$

and

$$\xi^2 = \frac{v_0}{36}\frac{1}{\chi_s - \chi}\left[\frac{b_A^2}{v_A\phi_A}\frac{\langle Z_A\rangle_z}{\langle Z_A\rangle_w} + \frac{b_B^2}{v_B\phi_B}\frac{\langle Z_B\rangle_z}{\langle Z_B\rangle_w}\right] \quad (3a)$$

Taking $\langle Z_i\rangle_z$ to be the z-averaged polymerization index for the Shultz–Zimm distribution, eq 3a reduces to

$$\xi^2 = \frac{v_0}{36}\frac{1}{\chi_s - \chi}\left[\frac{b_A^2}{v_A\phi_A}\frac{h_A+2}{h_A+1} + \frac{b_B^2}{v_B\phi_B}\frac{h_B+2}{h_B+1}\right] \quad (3b)$$

Thus, ξ can be determined without direct determination of $\langle Z_i\rangle_z$.

In Figure 1, typical SANS data from a miscible blend, in this case VBRD6/VBRH6 with a volume fraction of $\phi_{VBRD6} = 0.278$ and at room temperature, is displayed together with the best fitted line according to eq 1. A normalized deviation plot is also displayed in the lower half of Figure 1. This is to be contrasted with the SANS results of a phase-separated blend, in this case VBRD6/CisBR150k with 50/50 composition at room temperature which is displayed in Figure 2. The static structure factors for VBRD6/VBRH6 with $\phi_{VBRD6} = 0.375$ at various temperatures are shown in Figure 3 and for VBRD6/CisBR7k with $\phi_{VBRD6} = 0.092$ are shown in Figure 4. It is clear from Figures 3 and 4 that $S(q)$ decreases with

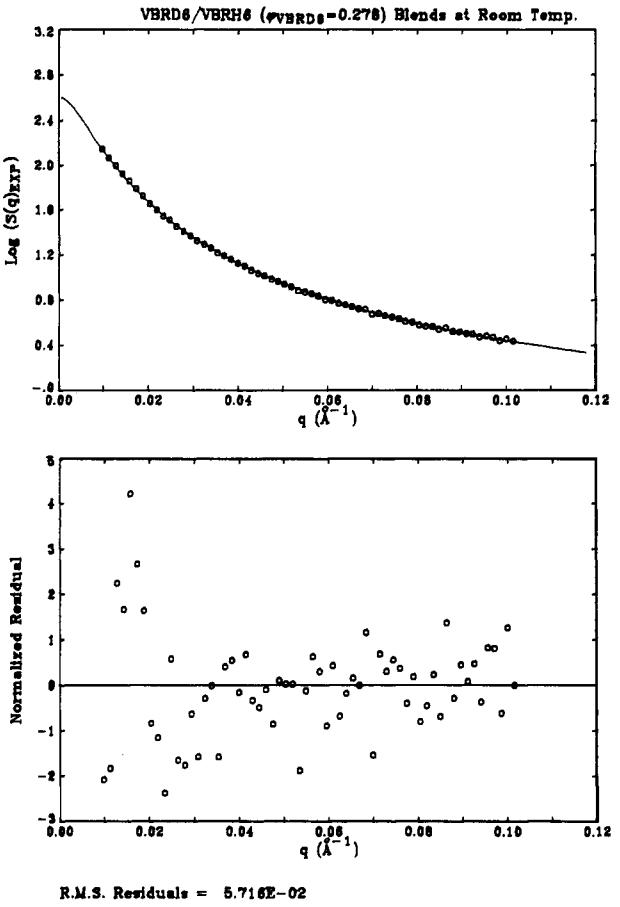

Figure 1. Normalized SANS intensity $S(q)$ of VBRD6/VBRH6 with volume fraction ϕ_{VBRD6} = 0.278 at room temperature is displayed in logarithmic scale as a function of scattering vector q together with the best fitted line according to eq 1. Normalized deviation is plotted in the lower half of the graph.

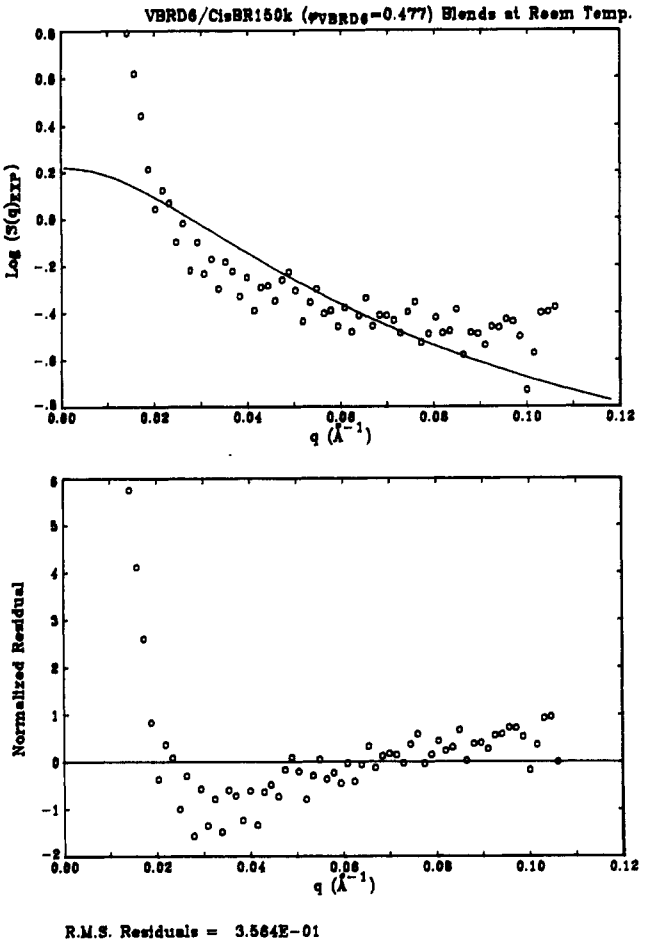

Figure 2. SANS data of an immiscible blend of VBRD6/CisBR150k with volume fraction ϕ_{VBRD6} = 0.477 at room temperature is displayed in the same fashion as Figure 1 to show the difference from a miscible blend.

increasing temperature for both series. This implies the existence of UCST's in both cases at temperatures below the room temperature. We will discuss the extrapolation to spinodal temperatures and the phase separation behavior later.

We will now discuss the fitted values of the statistical segment length and the base line and compare these values with the ones in the literature or predicted from independent measurements. The statistical segment length of 6.5 Å has been reported for medium vinyl polybutadiene (~43% 1,2-unit) at Θ condition and 6.56 Å for a high cis content (7% 1,2-unit) PB[18] also at Θ condition. These two values are essentially identical within experimental error. On the other hand, the statistical segment length for a 80% 1,2-unit PBD in bulk has been measured by SANS technique in low labeling concentration limit to be 6.88 Å.[19] Therefore, within the experimental error, we believe the use of a single adjustable parameter for both PB components (letting $b_A = b_B$) in this study is justified. Indeed, the final values for all b's were clustered around 6.5~6.9 Å with the extreme values of 6.23 and 7.11 Å. As for the base-line values, the difference between the fitted ones (range from +0.03 to 0.79) and the ones (0.85~1.01) calculated from pure polyisoprene and deuterated polybutadiene measurements according to the procedure used by Hayashi et al.[20] is negligible compared with the $S(q = 0)$ values which range from 35 to 728.

B. Interaction Parameter χ and Spinodal Temperature T_s. We have displayed the nonlinear regression fit for one set of the VBRD6/VBRH6 SANS data

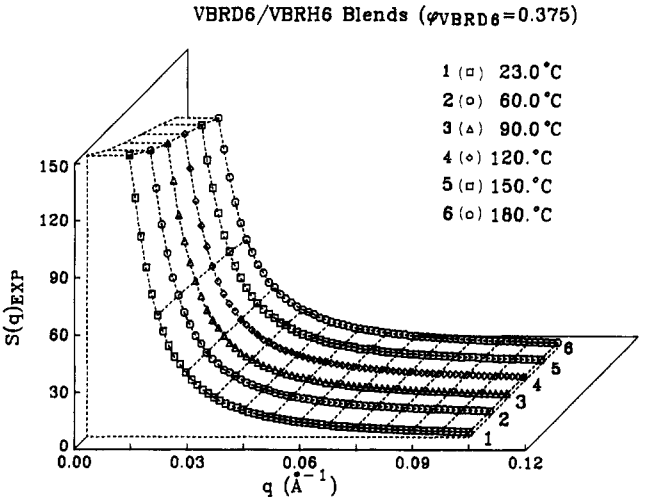

Figure 3. SANS data from the VBRD6/VBRH6 series with ϕ_{VBRD6} = 0.375 at various temperatures (show in the graph) is plotted as $S(q)$ vs q. Data are shifted along the 45° line for clarity.

in Figure 1 as discussed earlier. Actually, all SANS results from all four compositions of the VBRD6/VBRH6 series and the two compositions of the VBRD6/CisBR7k series at various temperatures can be fitted very nicely by eq 1. The interaction parameter, χ, zero wavenumber structure factor, $S(q = 0)$ and the correlation length, ξ, have been extracted according to eq 1–3 for all experimental conditions. Since polymer/polymer blends can be

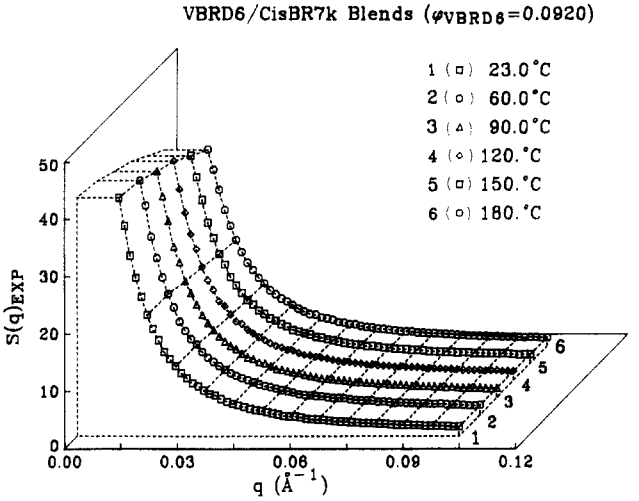

Figure 4. SANS data from the VBRD6/CisBR7k series with ϕ_{VBRD6} = 0.0920 at various temperatures is plotted as $S(q)$ vs q. Again data are shifted for clarity.

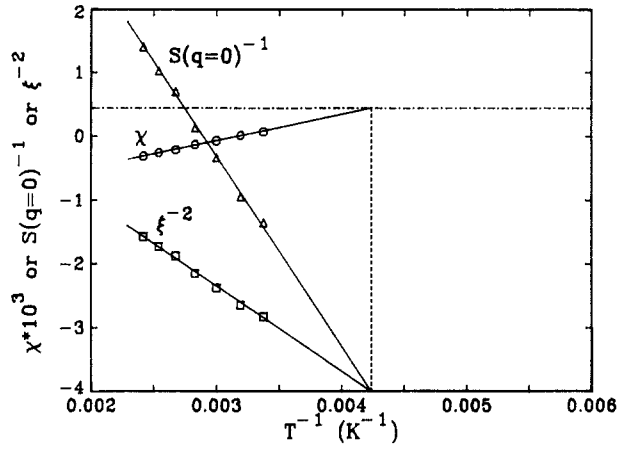

Figure 5. SANS results of χ [O], S (q = 0)$^{-1}$ [△], and ξ^{-2} [□] from nonlinear regression analysis for VBRD6/VBRH6 (ϕ_{VBRD6} = 0.474) are plotted against $1/T$. A dotted-and-broken (- · -) horizontal line displays the χ_s value for this system. Linear extrapolation are performed simultaneously for all three plots to obtain the spinodal temperature, T_s, in a consistent manner. In this case T_s = −37.2 °C. The scales labeled on the ordinate is for χ values. The scales for $S(q = 0)^{-1}$ is from 0.0 to 0.006 with a interval of 0.001 and for ξ^{-2} is from 0.0 to 0.00024 with an interval of 4 × 10^{-5} A^{-2}.

described by the mean-field theory,[17,21-24] spinodal or the critical temperature can be obtained through the extrapolation of χ, $S(q = 0)^{-1}$ or ξ^{-2} vs $1/T$ to $\chi = \chi_s$, $S(o)^{-1} \rightarrow 0$ or $\xi^{-2} \rightarrow 0$, respectively. Where χ_s is the χ at the spinodal temperature T_s as given by eq 2. In Figure 5, χ, $S(q = 0)^{-1}$, and ξ^{-2} are plotted vs $1/T$ for the VBRD6/VBRH6 (ϕ_{VBRD6} = 0.474) blend. T_s of −37.2 °C is obtained consistently from the extrapolations of all three sets of results. A similar procedure has been carried out for all data sets of both the VBRD6/VBRH6 and the VBRD6/CisBR7k series of blends. Results from VBRD6/CisBR7k at ϕ_{VBRD6} = 0.477 are displayed in Figure 6. Since a long extrapolation is required for this sample, the T_s obtained may not be very accurate. Nevertheless, with the help of simultaneous extrapolations of three sets of data, reasonable results can be obtained. The reason we cannot carry out the experiment close to T_s is because of the small yet positive coefficient of the $1/T$ dependence in χ that has lowered the spinodal temperatures beyond that readily accessible experimentally. In

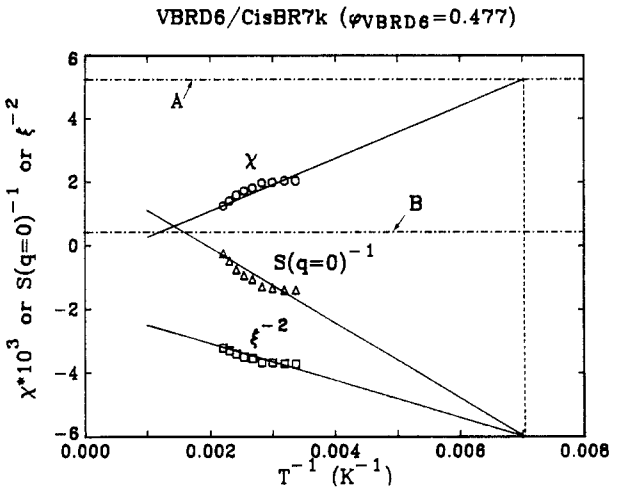

Figure 6. SANS results of χ [O], $S(q = 0)^{-1}$ [△], and ξ^{-2} [□] for VBRD6/CisBR7k (ϕ_{VBRD6} = 0.477) are plotted against $1/T$. A dotted-and-broken (- · -) horizontal line A displays χ_s value for this system. Simultaneous linear extrapolation from all three sets of data yields a spinodal temperature, T_s, of −131 °C. The scales of χ is labeled on the graph. The scales for $S(q = 0)^{-1}$ is from 0.0 to 0.06 with interval of 0.01 and for ξ^{-2} from 0.0 to 0.0024 with interval of 4 × 10^{-4} A^{-2}. A dotted-and-broken horizontal line B is also plotted which is the χ_s value of the VBRD6/CisBR150k (ϕ_{VBRD6} = 0.477) system.

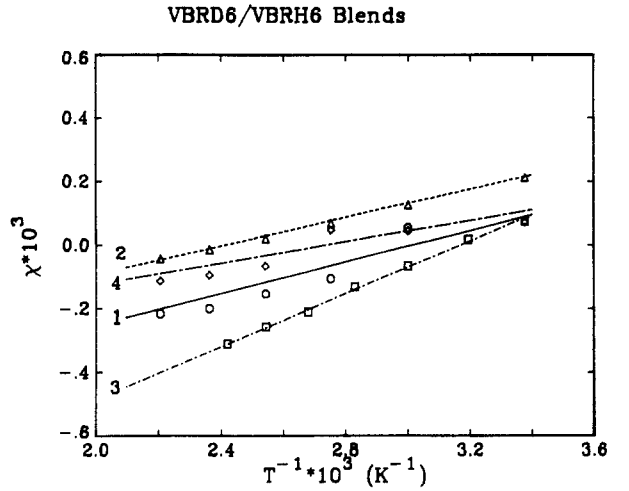

Figure 7. χ values of the VBRD6/VBRH6 series is plotted as a function of $1/T$: 1 [O], composition ϕ_{VBRD6} = 0.278; 2 [△], ϕ_{VBRD6} = 0.375; 3 [□], ϕ_{VBRD6} = 0.474; 4 [◇], ϕ_{VBRD6} = 0.677.

Figure 7, χ values obtained for the VBRD6/VBRH6 series blends are displayed as a function of $1/T$. The linear dependence of χ can be represented by

$$\chi = A + B/T \tag{4}$$

The coefficients A and B were obtained by the least-square fits and are listed in Table IV. Similar plots for the VBRD6/CisBR7k series are displayed in Figure 8. Again reasonably good $1/T$ dependence can be observed with a very small slope (or small coefficient B). The coefficients A and B obtained are also listed in Table IV.

CisBR7k and CisBR150K are quite different in molecular weight but very similar in microstructure. The χ_s value of the VBRD6/CisBR150K blend at ϕ_{VBRD6} = 0.477 was also calculated with eq 2 and is indicated in Figure 6 by the broken line B. If we neglect the molecular weight dependence of χ and the small microstructure difference, we can assume the VBRD6/CisBR150K blend has the same χ value as the VBRD6/CisBR7k blend. In this case, all the χ values are above χ_s at all temperatures

Table IV
Interaction Parameter, χ, and Its Coefficients

	ϕ_{VBRB6}	10^4A	B	$10^4\chi_s$	T_s, °C
VBRD6/VBRH6	0.278	−7.46 ± 1.69	0.248 ± 0.023	5.56	−82.7
	0.375	−5.39 ± 0.20	0.224 ± 0.003	4.76	−52.5
	0.474	−13.2 ± 0.2	0.417 ± 0.003	4.48	−37.2
	0.677	−4.61 ± 1.42	0.169 ± 0.017	5.10	−99.0
$\phi_{VBRD6,crit}$[a]	0.501	−13.2	0.417	4.46	(−37.0)
VBDR6/CisBR7k	0.092	0.507 ± 0.9	0.690 ± 0.01	40.8	−102
	0.477	−5.64 ± 0.5	0.825 ± 0.01	52.2	−131
$\phi_{VBRD6,crit}$[a]	0.172	−0.765	0.718	38.0	(−87.9)
VBRD6/CisBR150k	0.477			4.32	(555)

[a] A and B values for $\chi(\phi_A = \phi_{A,crit})$ are estimated values from experimentally obtained values listed in this table.

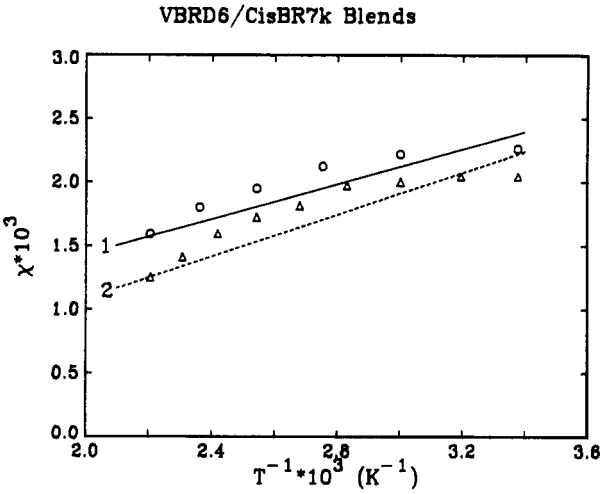

Figure 8. χ values of the VBRD6/CisBR7k series is plotted as a function of $1/T$: 1 [○], composition ϕ_{VBRD6} = 0.0920; 2 [△], ϕ_{VBRD6} = 0.477.

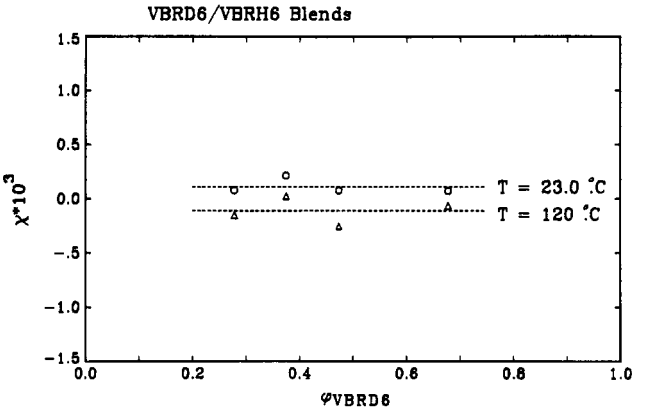

Figure 9. χ values of the VBRD6/VBRH6 blends at 23 °C [○] and at 120 °C [△] are plotted against ϕ_{VBRD6}. Within experimental error, no obvious composition dependence of χ has been observed.

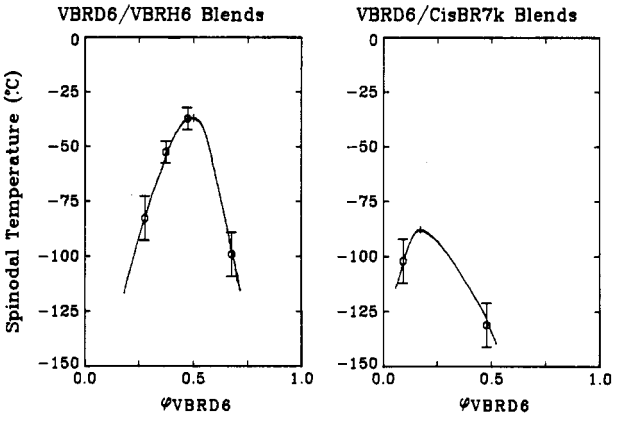

Figure 10. Phase diagrams of the VBRD6/VBRH6 system and the VBRD6/CisBR7k system are presented. Experimental spinodal points [○] and the calculated critical point from Table IV [+] are shown together with a curve drawn through all spinodal points.

below ca. 600 °C. Then, phase separation is certainly expected for the VBRD6/CisBR150k series at room temperature, which is consistent with our observation.

It should be noted that all the χ values obtained for VBRD6/CisBR7k are positive as indicated in Figure 8. On the other hand, some χ values obtained for VBRD6/VBRH6 and indicated in Figure 7 are negative which would suggest the existence of some kind of specific interaction between two polymers in case of homopolymer blends. However, these negative χ values are not due to the specific interaction between the deuterated and protonated polymers, but to the copolymer effect as will be discussed in section IIIC.

If we examine closely the χ vs $1/T$ results for either Figure 6 or Figure 8, we can see downward curvature in the VBRD6/CisBR7k series. This downward curvature is most likely due to inaccuracies in our experiment and our data analysis because we are trying to measure very subtle temperature effects at temperatures that are far away from the spinodal temperature. However, we cannot rule out the other possibility that this system may become more compatible again at very low temperature.

In Figure 9, the composition dependence of χ for VBRD6/VBRH6 at 23 and 120 °C is displayed. Within the experimental error and the limited data set, we do not see any obvious composition dependence of χ.

The phase diagram with the experimentally obtained spinodal temperatures is displayed in Figure 10 for both VBRD6/VBRH6 and VBRD6/CisBR7k systems. The critical composition, ϕ_c, is determined according to

$$\phi_{C,A} = (v_B\langle Z_B\rangle_w)^{1/2}/[(v_A\langle Z_A\rangle_w)^{1/2} + (v_B\langle Z_B\rangle_w)^{1/2}] \quad (5)$$

This equation is derived in Appendix B. The critical temperature, T_c, is located by interpolating the χ value at $\phi_{C,A}$ and by setting $\chi(\phi_{C,A}, T) = \chi_s$ ($\phi_A = \phi_{C,A}$). The rest of the curve is drawn roughly through the measured spinodal temperatures. The gross asymmetry of the phase diagram of the VBRD6/CisBR7k blend is due to the molecular weight difference between VBRD6 (M_n = 134 × 10^3)and CisBR7k (M_n = 6.9 × 10^3).

C. Separation of Microstructure and Isotope Labeling Effects. Besides the isotope effect that could cause incompatibility,[3] the microstructure effect has to be properly accounted for in order to understand the phase behavior of rubber/rubber blends. We will make an attempt in this paper to separate isotope effect from microstructure effect by using theoretical calculations of ten Brinke, Karasz, and MacKnight for random copolymers.[4] If we

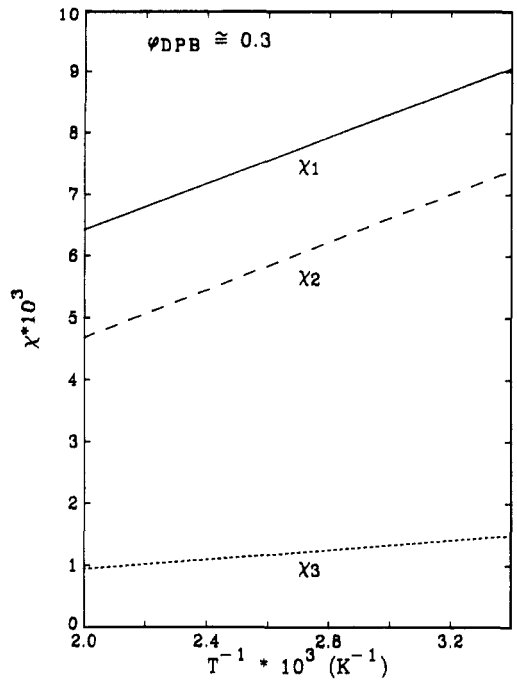

Figure 11. χ_1, χ_2, and χ_3 obtained as in section IIIC are presented as a function of $1/T$.

define deuterated 1,2-butadiene, deuterated 1,4-butadiene, protonated 1,2-butadiene, and protonated 1,4-butadiene monomers as A, B, C, and D, respectively, then, for a blend of A–B copolymer with C–D copolymer, the free energy of mixing can be written as

$$\frac{\Delta F}{RT} = (\phi_1/N_1) \ln \phi_1 + (\phi_2/N_2) \ln \phi_2 + \phi_1\phi_2\chi_{blend} \quad (6)$$

with

$$\chi_{blend} = xy\chi_{AC} + (1-x)y\chi_{BC} + x(1-y)\chi_{AD} + (1-x)(1-y)\chi_{BD} - x(1-x)\chi_{AB} - y(1-y)\chi_{CD} \quad (7)$$

where x is the number fraction of A in A–B copolymer and y is the number fraction of C in C–D copolymer. x and y refer to the number fraction of repeat units in the lattice theory of blends. We equated number fractions to volume fractions for this work.

By neglecting the difference between *trans*- and *cis*-1,4 polybutadiene and assuming polybutadiene is a simple random copolymer, we should be able to obtain all six χ parameters if we have six sets of data for blends with different microstructure variations. We do not have six sets of data. Nontheless using the data from Bates et al.[3] and making a few assumptions about the interaction parameters, we shall demonstrate a scheme of separating various interaction parameters.

First, let us assume $\chi_{AC} = \chi_{BD} \equiv \chi_3$. This assumption implies identical isotope effect between 1,2-pairs and between 1,4-pairs of different isotopes. Without knowledge of the exact intermolecular potential energy function between two isotopically labeled microstructure pairs the severity of this assumption cannot be assessed. Once we have made the above assumption, we can then assume $\chi_{AB} = \chi_{CD} \equiv \chi_1$ and $\chi_{AD} = \chi_{BC} \equiv \chi_2$. These two assumptions imply that pure microstructure effect (interaction between either protonated or deuterated 1,2- and 1,4-butadiene pairs) is independent of isotope used and consequently that the cross (isotope labeled) microstructure effect is independent of which one of the two monomers is labeled. Actually, these two assumptions are implied from the previous assumption that identical isotope effects prevail between 1,2-pairs and 1,4-pairs.

Table V
Individual Interaction Parameters χ_1, χ_2, and χ_3 as the Solutions of Eq 8 and 9 for Blend Composition of $\phi_{PBD} \cong 0.3$

	10^4A	B
χ_1 (H1,2 ↔ H1,4) (D1,2 ↔ D1,4)	26.9	1.87
χ_2 (H1,2 ↔ D1,4) (D1,2 ↔ H1,4)	8.24	1.93
χ_3 (H1,2 ↔ D1,2) (H1,4 ↔ D1,4)	1.68	0.39

We are now in a position to calculate the three interaction parameters χ_1, χ_2, and χ_3 for three sets of PBD/PBH blends. As noted before, we have two sets of χ data from this study as listed in Table IV and we will also employ the literature value of Bates et al.,[3] which was reported for a PBD/PBH system with 11% of 1,2-unit for both components and with $\phi_{PBD} = 0.31$. The χ data used in this calculation should be obtained for the same volume fraction of deuterated polybutadiene for the three sets of blends. Unfortunately, χ data in our experiment were not measured at the same composition as the one reported by Bate's et al.[3] Therefore, we have used the measured χ values at $\phi_{VBRD6} = 0.278$ for the VBRD6/VBRH6 blend and interpolted χ values at $\phi_{VBRD6} = 0.24$ (interpolated value from $\phi_{VBRD6} = 0.0920$ and 0.477 data) for the VBRD6/CisBR7k blend. Thus, the three sets of χ data used in the following calculation were based on three blends with some differences in their volume fractions, i.e., 0.278 for VBRD6/VGbRH6, 0.24 for VBRD6/CisBR7k, and 0.31 for PBD/PBH by Bates et al.[3] However, the change of χ values by small differences of the volume fraction is considered to be very small as suggested by Figures 8 and 9 and may be comparable to the errors in the evaluation of χ_1, χ_2, and χ_3.

Thus, three simultaneous equations can be obtained from eq 7 as

$$\chi(\text{VBRD6/VBRH6}) = -0.451\chi_1 + 0.454\chi_2 + 0.546\chi_3 \quad (8a)$$

$$\chi(\text{VBRD6/CisBR7k}) = -0.307\chi_1 + 0.610\chi_2 + 0.390\chi_3 \quad (8b)$$

$$\chi(\text{Bates et al.}) = -0.196\chi_1 + 0.196\chi_2 + 0.804\chi_3 \quad (8c)$$

With the temperature dependences of χ given by

$$\chi(\text{VBRD6/VBRH6}) = -7.46 \times 10^{-4} + 0.248/T \quad (\phi = 0.278) \quad (9a)$$

$$\chi(\text{VBRD6/CisBR7k}) = -2.57 \times 10^{-4} + 0.758/T \quad (\phi = 0.24) \quad (9b)$$

$$\chi(\text{Bates et al.}) = 2.3 \times 10^{-4} + 0.326/T \quad (\phi = 0.31) \quad (9c)$$

Values of χ_1, χ_2, and χ_3 obtained for eq 8 and 9 are displayed in Figure 11 as a function of $1/T$. The corresponding coefficients are listed in Table V.

D. Predictions and Implications. In this section we will test the above method that separates χ into three interactions, χ_1, χ_2, and χ_3, by comparing the predicted χ values with measured ones of an independent set of SANS data. This set of data was obtained from a blend of an anionically polymerized deuterated polybutadiene, H-19 (with $M_n = 71 \times 10^3$, $M_w/M_n \sim 1.0$, and 28% of 1,2-unit), and a protonated polybutadiene, H-16 (with $M_n = 281 \times 10^3$, $M_w/M_n \sim 1.01$, and 40% of 1,2-unit) at $\phi_{PBD} = 0.757$. SANS measurement and data analysis have been carried out with identical procedures as described

before. In Figure 12, χ values obtained from SANS measurements of this H-19/H-16 blend are displayed as a function of $1/T$ together with the predicted values (solid line) that were calculated according to eq 7 and Table V. Although the predicted numbers are slightly lower than the experimental values, considering the assumptions and errors involved in the calculation, in this analysis, in sample preparation, and in SANS experiments, this agreement may be considered to be excellent.

We should point out that the main contribution for miscibility in a blend of a A–B copolymer with a C–D copolymer is due to the interaciton between the intramolecular pairs of A/B and C/D which has a negative coefficient as indicated in eq 7. Actually, in order to maximize this negative contribution to the total interaction, χ_{blend}, copolymers of equal constituents ($x_A = x_B = 0.5$, $y_C = y_D = 0.5$) should be used. This is certainly consistent with the original idea of ten Brinke, Karasz, and MacKnight. More specifically, for deuterated polybutadiene/polybutadiene blends, irrespective of the isotope effect, maximum miscibility can be achieved by using 50% 1,2 content for both components. This is obvious by examining the coefficients in eq 9a, 9b, and 9c for the three series of blends used and clearly is reflected from the corresponding T_s for the three series.

If we examine Figure 7 again with these intramolecular interactions in mind, then it becomes clear why negative χ's have been obtained for deuterated polybutadiene/protonated polybutadiene blends that lack any specific attractive interaction.

IV. Conclusion

In this work, we have presented results for deuterated polybutadiene/protonated polybutadiene blends with various microstructures and compositions. We found that the static structure factor $S(q)$ from the SANS experiments for miscible (at room temperature) blends can be well represented by the RPA calculation. From that analysis the interaction parameter, χ/v_0, correlation legnth, ξ, and zero wavenumber structure factor, $S(q = 0)$, can be extracted. The spinodal temperature can be obtained through extrapolation. Phase diagrams for these polymer blends can be constructed, and they all show UCST behavior.

Interaction parameter, χ_{blend}, of a blend of any given composition can be represented by a simple $A + B/T$ functional form. If we neglect the molecular weight dependence of χ, then the χ_{blend} can be separated into three interaction terms. These three interaction parameters χ_1, χ_2 and χ_3 represent binary interaction between the same isotopically labeled (with deuterated or protonated) 1,2-unit and 1,4-unit, the opposite isotopically labeled 1,2-unit and 1,4-unit, and the opposite isotopically labeled 1,2-unit and 1,2-unit or 1,4-unit and 1,4-unit, respectively. Reasonable success has been demonstrated by comparing the measured χ_{blend} with predicted χ_{blend} (from previously obtained χ_1, χ_2, and χ_3) for an independent set of PBD/PBH blend.

Although we have assumed that (1) isotope effect is identical between 1,2-pairs and 1,4-pairs, (2) the pure microstructure effect is independent of isotope used, and (3) the cross microstructure effect is independent of which one of the two monomers is labeled, nevertheless, we think the random copolymer theory of ten Brinke, Karasz, and MacKnight[4] works well for our case. The intramolecular interaction parameter, χ_1, which gives a negative contribution to the total χ_{blend} is actually responsible for the negative sign of the χ_{blend} (see Figure 7). It is generally accepted that anionically polymerized polybutadiene has a microstructure (1,2 versus 1,4) distribution close to random,[25] but we think more experiments are needed to eliminate the above assumptions in the future and also to incorporate the sequence distribution suggested by Balazs et al.,[26,27] especially for polyisoprene blends.

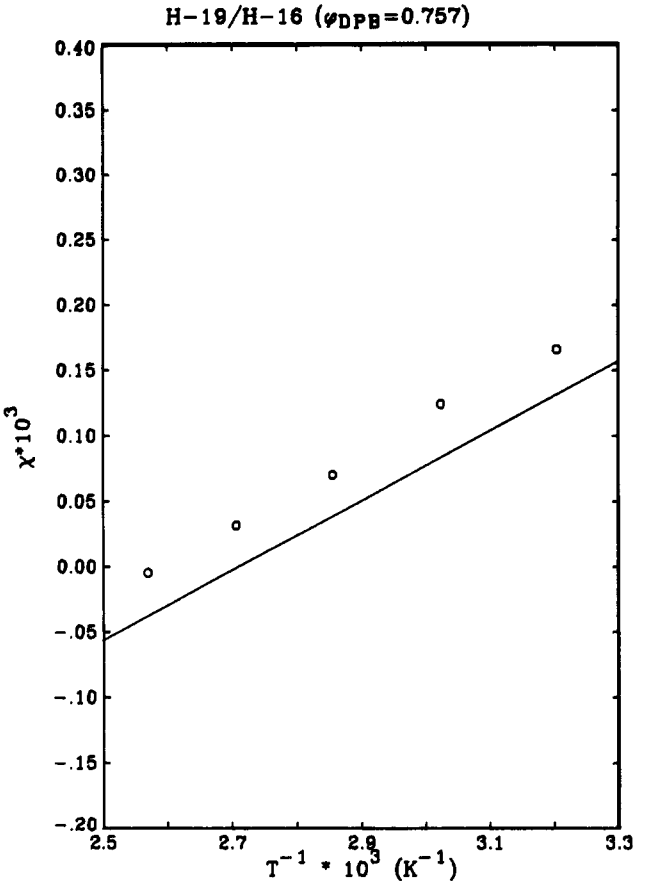

Figure 12. Measured χ values [O] for the H-19/H-16 (PBD/PBH) series at a volume fraction of 0.757 of H-19 (PBD) is plotted against $1/T$ together with the predicted χ values in solid line which was calculated by using eq 7 and the χ_1, χ_2, and χ_3 values from Table V.

Appendix A. The Effect of Polydispersity

By following Hong and Noolandi[12] the RPA results for a two-component blend system can be written as

$$S(q) = k_N/\left[\frac{1}{\phi_A v_A \langle Z_A g_D(x_A)\rangle_w} + \frac{1}{\phi_B v_B \langle Z_B g_D(x_B)\rangle_w} - \frac{2\chi}{v_0}\right] \quad \text{(A1)}$$

where $\langle\ \rangle_w$ represents weight average and $g_D(x_i)$ is the Debye function

$$g_D(x_i) = \frac{2}{x_i^2}[\exp(-x_i) - 1 + x_i] \quad \text{(A2)}$$

with $x_i = Z_i b_i^2 q^2/6 = q^2 R_{gi}^2$, where b_i is the statistical segment length and R_{gi} is the radius of gyration of the ith component, respectively.

If we use the Shultz–Zimm[10] molecular weight distribution, then

$$n(Z_i) = \frac{\lambda^{h_i}}{\Gamma(h_i)} Z_i^{h_i - 1} \exp(-\lambda Z_i) \quad \text{(A3)}$$

The number-average, weight average, and z-average degree of polymerization can be written as in (A4a), (A4b), and

(A4c), respectively.

$$\langle Z_i\rangle_n = \frac{\int_0^\infty Z_i\, n(Z_i)\, dZ_i}{\int_0^\infty n(Z_i)\, dZ_i} = \frac{h_i}{\lambda} \tag{A4a}$$

$$\langle Z_i\rangle_w = \frac{\int_0^\infty Z_i^2\, n(Z_i)\, dZ_i}{\int_0^\infty Z_i\, n(Z_i)\, dZ_i} = \frac{(h_i+1)h_i/\lambda^2}{h_i/\lambda} = \frac{h_i+1}{\lambda} \tag{A4b}$$

$$\langle Z_i\rangle_z = \frac{\int_0^\infty Z_i^3\, n(Z_i)\, dZ_i}{\int_0^\infty Z_i^2\, n(Z_i)_i\, dZ_i} = \frac{(h_i+2)(h_i+1)h_i/\lambda^3}{(h_i+1)h_i/\lambda^2} = \frac{h_i+2}{\lambda} \tag{A4c}$$

One can also obtain

$$\frac{\langle Z_i\rangle_w}{\langle Z_i\rangle_n} = \frac{h_i+1}{h_i}$$

$$\frac{\langle Z_i\rangle_z}{\langle Z_i\rangle_n} = \frac{h_i+2}{h_i}$$

$$h_i = \frac{1}{\langle Z_i\rangle_w/\langle Z_i\rangle_n - 1} \tag{A5}$$

The weight fraction distribution W_p can be written as

$$W_p(Z_i) \equiv \frac{Z_i n(Z_i)}{\int Z_i\, n(Z_i)\, dZ_i} = \frac{Z_i n(Z_i)}{h_i/\lambda} = \frac{\lambda^{h_i+1}}{\Gamma(h_i+1)} Z_i^{h_i} \exp(-\lambda Z_i) \tag{A6}$$

and

$$\langle Z_i g_D(x_i)\rangle_w = \int_0^\infty Z_i\, g_D(x_i)\, W_p(Z_i)\, dZ_i$$

$$= \frac{1}{(b_i^2q^2/6)^2}\int_0^\infty Z_i \frac{2}{Z_i^2}\left\{\exp\left(-\frac{b_i^2q^2}{6}Z_i\right) - 1 + \frac{b_i^2q^2}{6}Z_i\right\} \times \left\{\frac{\lambda^{h_i+1}}{\Gamma(h_i+1)} Z_i^{h_i}\exp(-\lambda Z_i)\right\} dZ_i$$

$$= \frac{2}{(b_i^2q^2/6)^2}\frac{\lambda^{h_i+1}}{\Gamma(h_i+1)}\int_0^\infty \left\{Z_i^{h_i-1}\exp\left[-\left(\lambda + \frac{b_i^2q^2}{6}\right)Z_i\right] - Z_i^{h_i-1}\exp(-\lambda Z_i) + \frac{b_i^2q^2}{6}Z_i^{h_i}\exp(-\lambda Z_i)\right\} dZ_i$$

$$= \frac{2}{\langle x_i\rangle_n^2}\frac{\lambda^{h_i+1}}{\Gamma(h_i+1)}\langle Z_i\rangle_n^2\left\{\frac{\Gamma(h_i)}{\left(\lambda + \frac{\langle x_i\rangle_n}{\langle Z_i\rangle_n}\right)^{h_i}} - \frac{\Gamma(h_i)}{\lambda^{h_i}} + \frac{\langle x_i\rangle_n}{\langle Z_i\rangle_n}\frac{\Gamma(h_i+1)}{\lambda^{h_i+1}}\right\}$$

$$= \langle Z_i\rangle_n \frac{2}{\langle x_i\rangle_n^2}\left\{\left(\frac{\lambda}{\lambda + \lambda\langle x_i\rangle_n/h_i}\right)^{h_i} - 1 + \langle x_i\rangle_n\right\}$$

$$= \langle Z_i\rangle_n \frac{2}{\langle x_i\rangle_n^2}\left[\left(\frac{h_i}{h_i + \langle x_i\rangle_n}\right)^{h_i} - 1 + \langle x_i\rangle_n\right]$$

$$= \langle Z_i\rangle_n \langle g_D(x_i)\rangle_w \tag{A7}$$

with

$$\langle g_D(x_i)\rangle_w \equiv \frac{2}{\langle x_i\rangle_n^2}\left[\left(\frac{h_i}{h_i + \langle x_i\rangle_n}\right)^{h_i} - 1 + \langle x_i\rangle_n\right] \tag{A8}$$

This form was first derived by Mori, Tanaka, Hasegawa, and Hashimoto.[15] Equation 1a in the text can be obtained by substitute eq A8 into eq A1. Notice that in the limiting case, conventional results can be recovered from (A8). For example, (1) Monodisperse limit: The function $F(h_i) \equiv [h_i/(h_i + \langle x_i\rangle)_n]^{h_i}$ can be rewritten as

$$\ln F(h_i) = h_i \ln\left(\frac{1}{1 + \langle x_i\rangle_n/h_i}\right)$$

as

$$\frac{M_w}{M_n} \to 1,\ h_i \to \infty,\ \text{and}\ \frac{\langle x_i\rangle_n}{h_i} \to 0$$

$$\ln F(h_i) = h_i\left[-\left(\frac{\langle x_i\rangle_n}{h_i}\right) + \dots\right] \cong -\langle x_i\rangle_n$$

or

$$\lim_{M_w/M_n\to 1}\left(\frac{h_i}{h_i + \langle x_i\rangle_n}\right)^{h_i} = e^{-\langle x_i\rangle_n} \tag{A9}$$

This recovers the original Debye function.

(2) Small q limit: let $f(\langle x_i\rangle_n) \equiv [h_i/(h_i + \langle x_i\rangle_n)]^{h_i}$ if we make a Taylor expansion with respect to $\langle x_i\rangle_n$ and keep three orders of $\langle x_i\rangle_n$ in the expansion, then

$$f(\langle x_i\rangle_n) = 1 - \langle x_i\rangle_n + \frac{1}{2}\left(h_i + \frac{1}{h_i}\right)\langle x_i\rangle_n^2 - \frac{1}{6}\left(\frac{h_i+1}{h_i}\right)\times\left(\frac{h_i+2}{h_i}\right)\langle x_i\rangle_n^3$$

$$= 1 - \langle x_i\rangle_n + \frac{1}{2}\frac{\langle Z_i\rangle_w}{\langle Z_i\rangle_n}\langle x_i\rangle_n^2 - \frac{1}{6}\frac{\langle Z_i\rangle_w}{\langle Z_i\rangle_n}\frac{\langle Z_i\rangle_z}{\langle Z_i\rangle_n}\langle x_i\rangle_n^3 \tag{A10}$$

Substitute eq A10 into eq A8, then we obtain

$$\langle g_D(x_i)\rangle_w = \frac{\langle Z_i\rangle_w}{\langle Z_i\rangle_n}\left[1 - \frac{1}{3}\frac{\langle Z_i\rangle_z}{\langle Z_i\rangle_n}\langle x_i\rangle_n\right]$$

and

$$[\phi_i v_i \langle Z_i\rangle_n \langle g_D(x_i)\rangle_w]^{-1} \cong \frac{1 + \frac{1}{3}\frac{\langle Z_i\rangle_z}{\langle Z_i\rangle_n}\frac{1}{6}\langle Z_i\rangle_n b_i^2 q^2}{\phi_i v_i \langle Z_i\rangle_w} \tag{A11}$$

Combining this equation and eq 1a from the text, we obtain

$$S(q) = k_N/\left\{\left(\frac{1}{\phi_A v_A\langle Z_A\rangle_w} + \frac{1}{\phi_B v_B\langle Z_B\rangle_w} - \frac{2\chi}{v_0}\right) + \frac{1}{18\phi_A\phi_B}\times\left[\phi_A\phi_B\left(\frac{\langle Z_A\rangle_z}{\langle Z_A\rangle_w}\frac{b_A^2}{\phi_A v_A} + \frac{\langle Z_B\rangle_z}{\langle Z_B\rangle_w}\frac{b_B^2}{\phi_B v_B}\right)q^2\right]\right\} \tag{A12}$$

This is the same as given in ref 14 by Joanny.

Appendix B. Critical Composition for a Polydispersed System

Spinodal point can be obtained from eq A12 at $S(q = 0) \to \infty$

$$\chi_{spinodal}(\phi_A) \equiv \chi_s = \frac{v_0}{2}\left[\frac{1}{v_A\langle Z_A\rangle_w\phi_A} + \frac{1}{v_B\langle Z_B\rangle_w(1-\phi_A)}\right] \tag{B1}$$

at critical point $\partial^3 F(\phi_A)/\partial\phi_A{}^3 = 0$ or $\partial\chi_s(\phi_A)/\partial\phi_A = 0$.

$$\frac{\partial\chi_s(\phi_A)}{\partial\phi_A} = 0 = \frac{v_0}{2}\left(\frac{-1}{v_A\langle Z_A\rangle_w\phi_A{}^2} + \frac{1}{v_B\langle Z_B\rangle_w(1-\phi_A)^2}\right)$$

and

$$\phi_{A,critical} = \frac{(v_B\langle Z_B\rangle_w)^{1/2}}{(v_A\langle Z_A\rangle_w)^{1/2} + (v_B\langle Z_B\rangle_w)^{1/2}} \quad \text{(B2)}$$

This is eq 5 in the text.

References and Notes

(1) *Handbook of Elastomers*; Bhowmick, A. K., Stephens, H. L., Eds.; Marcel Dekker: New York, 1988.
(2) For example: Shibayama, M.; Yang, H.; Stein, R. S.; Han, C. C. *Macromolecules* **1985**, *18*, 2179.
(3) Bates, F. S.; Dierker, S. B.; Wignall, G. D. *Macromolecules* **1986**, *19*, 1938.
(4) ten Brinke, G.; Karasz, F. E.; MacKnight, W. J. *Macromolecules* **1983**, *16*, 1827.
(5) Kambour, R. P.; Bendler, J. T.; Bopp, R. C. *Macromolecules* **1983**, *16*, 753.
(6) Paul, D. R.; Barlow, J. W. *Polymer* **1984**, *25*, 487.
(7) Glinka, C. J.; Rowe, J. M.; LaRock, J. G. *J. Appl. Crystallogr.* **1986**, *19*, 427.
(8) Glinka, C. J., private communication.
(9) de Gennes, P.-G. *Scaling Concepts in Polymer Physics*; Cornell University Press: New York, 1979.
(10) Peebles, L. H., Jr. *Molecular Weight Distributions in Polymers*; Interscience: New York, 1970.
(11) Korstorz, G.; Lovesey, G. *Treatise on Materials Science and Technology*; Neutron *Scattering*; Academic Press: New York, 1979; Vol. 15, pp 5–8.
(12) Hong, K. M.; Noolandi, J. *Polym. Commun.* **1984**, *25*, 265.
(13) Rameau, A.; Gallot, Y.; Marie, P.; Farnoux, B. *Polymer* **1989**, *30*, 386.
(14) Ionescu, L.; Picot, C.; Duval, M.; Puplessix, R.; Benoit, H.; Cotton, J. P. *J. Polym. Sci., Poly. Phys. Ed.* **1981**, *19*, 1019.
(15) Mori, K.; Tanaka, H.; Hasegawa, H.; Hashimoto, T. *Polymer*, in press.
(16) Joanny, J. F. *C. R. Hebd. Seances Acad. Sci.* **1978**, *286B*, 89.
(17) Han, C. C.; Bauer, B. J.; Clark, J. C.; Muroga, Y.; Matsushita, M.; Okada, M.; Tran-Cong, Q.; Chang, T.; Sanchez, I. C. *Polymer* **1988**, *29*, 2002.
(18) Mays, J.; Hadjichristidis, N.; Fetters, L. J. *Macromolecules* **1984**, *17*, 2723.
(19) Sakurai, S.; Hasegawa, H.; Hashimoto, T.; Han, C. C., paper in preparation.
(20) Hayashi, H.; Flory, P. J.; Wignall, G. D. *Macromolecules* **1983**, *16*, 1328.
(21) Joanny, J. F. *J. Phys. A* **1978**, *11*, L117.
(22) de Gennes, P.-G. *J. Phys. Lett.* **1977**, *38*, L441.
(23) Binder, K. *J. Chem. Phys.* **1983**, *79*, 6387.
(24) Han, C. C. *Molecular Conformation and Dynamics of Macromolecules in Condensed Systems*; Nagasawa, M., Ed.; Elsevier: New York, 1988.
(25) Fetters, L. J., private communication.
(26) Balazs, A. C.; Sanchez, I. C.; Epstein, I. R.; Karasz, F. E.; MacKnight, W. J. *Macromolecules* **1985**, *18*, 2188.
(27) Balazs, A. C.; Karasz, F. E.; MacKnight, W. J.; Ueda, H.; Sanchez, I. C. *Macromolecules* **1985**, *18*, 2784.

Registry No. PBD, 9003-17-2; neutron, 12586-31-1.

Phase Separation Dynamics of Rubber/Epoxy Mixtures

Hak-soo Lee and Thein Kyu*

Center for Polymer Engineering, University of Akron, Akron, Ohio 44325.

Received March 20, 1989; Revised Manuscript Received June 16, 1989

ABSTRACT: Time-resolved light scattering has been employed to investigate the kinetics of phase separation in mixtures of carboxyl-terminated butadiene–acrylonitrile copolymer (CTBN) and diglycidyl ether bisphenol A (DGEBA) epoxy oligomers. The CTBN/DGEBA mixture reveals an upper critical solution temperature (UCST); i.e., the mixture phase separates upon cooling but reverts to a single phase upon heating. Several temperature- (T-) quench experiments with various quenched depths were undertaken on a 20 wt % CTBN mixture. The time evolution of scattering halo was subsequently followed as a function of quenched depth. At deep quenches, the phase separation process has been dominated by spinodal decomposition (SD). The general trend of SD is nonlinear in character. The evolution of the maximum wavenumber (q_m) and the corresponding maximum intensity (I_m) obey the power law ($q_m \sim t^{-\varphi}$ and $I_m \sim t^{\psi}$). The exponent φ exhibits quench depth dependence with the value varying from 1/6 to 1/3. The results were further tested with the dynamic scaling laws.

Introduction

Rubber-modified plastics have been the subject of continued interest in the field of polymer alloys. Thermoset epoxy resins are generally known to be brittle. Hence, the utilization of epoxy as a neat resin is not practical in many industrial applications. However, a slight addition of rubbery components into epoxy resins has been shown to improve mechanical properties of the materials, particularly toughness.[1] Since then, there have been numerous studies in the literature on the rubber-modified epoxies.[2–8]

It has been realized that the extent of improvement critically depends upon the size of rubbery particles, their dispersion, and interfacial adhesion between the dispersed rubbery phase and the matrix. The final morphology of the cured system depends on the competition between the cross-linking reaction and phase decomposition during curing. The understanding of reaction kinetics and phase separation dynamics is of crucial importance in order to achieve an optimum phase structure. In this study, the kinetic behavior of CTBN/DGEBA oligomer mixtures has been explored exclusively without adding any cross-linking agents.

Experimental Section

The epoxy resin used in this study was a diglycidyl ether Bisphenol A (DGEBA) supplied by the Shell Co. (Epon 828, $M_n \cong 380$). The elastomeric modifier, provided by the B.F. Goo-

* To whom correspondence should be addressed.

0024-9297/90/2223-0459$02.50/0